



HAL
open science

**Hyphenation of ultra-high performance supercritical
fluid chromatography with atmospheric pressure
chemical ionisation high resolution mass spectrometry:
Part 2. Study of chromatographic and mass
spectrometry parameters for the analysis of natural
non-polar compounds**

Johanna Duval, Cyril Colas, Pascal Bonnet, Eric Lesellier

► **To cite this version:**

Johanna Duval, Cyril Colas, Pascal Bonnet, Eric Lesellier. Hyphenation of ultra-high performance supercritical fluid chromatography with atmospheric pressure chemical ionisation high resolution mass spectrometry: Part 2. Study of chromatographic and mass spectrometry parameters for the analysis of natural non-polar compounds. *Journal of Chromatography A*, 2019, 1596, pp.199 - 208. 10.1016/j.chroma.2019.03.018 . hal-03484950

HAL Id: hal-03484950

<https://hal.science/hal-03484950v1>

Submitted on 20 Dec 2021

HAL is a multi-disciplinary open access archive for the deposit and dissemination of scientific research documents, whether they are published or not. The documents may come from teaching and research institutions in France or abroad, or from public or private research centers.

L'archive ouverte pluridisciplinaire **HAL**, est destinée au dépôt et à la diffusion de documents scientifiques de niveau recherche, publiés ou non, émanant des établissements d'enseignement et de recherche français ou étrangers, des laboratoires publics ou privés.



Distributed under a Creative Commons Attribution - NonCommercial 4.0 International License

1
2 **Hyphenation of ultra-high performance supercritical fluid chromatography**
3 **with atmospheric pressure chemical ionisation high resolution mass**
4 **spectrometry: Part 2. Study of chromatographic and mass spectrometry**
5 **parameters for the analysis of natural non-polar compounds.**

6
7 Johanna Duval, Cyril Colas, Pascal Bonnet, Eric Lesellier*

8 * Corresponding author: eric.lesellier@univ-orleans.fr

9 University of Orléans, CNRS, ICOA, UMR 7311, 45 067 Orléans, France.

10

11 **Abstract**

12
13 An analytical method based on Ultra-High-Performance Sub/Supercritical Fluid
14 Chromatography (UHPSFC) coupled with High-Resolution Mass Spectrometry (HR-MS)
15 equipped with an Atmospheric Pressure Chemical Ionisation source (APCI-Q-TOF-HRMS)
16 was developed for the screening of various compounds in oily samples. The hyphenation was
17 achieved using a hybrid UHPSFC system for the vegetable oil analysis, mainly composed of
18 fatty acids, diacylglycerols, triacylglycerols but containing also some minor bioactive
19 compounds. No split was used with this ionisation source in this optimized configuration,
20 allowing the introduction of all compounds in the mass spectrometer, ensuring a better
21 sensitivity. This configuration is preserving peak shapes and efficiency because the dead
22 volume of this interface is optimized by the supplier for the hyphenation with open cell
23 detectors such as Evaporative Light Scattering Detector (ELSD) or MS detectors. The
24 influence of analytical conditions (UHPSFC and APCI parameters) on MS response was
25 studied to understand the behaviour of analytes in UHPSFC-APCI-MS. The tested parameters
26 were: the corona discharge value, the nebulising gas pressure, the drying gas flow rate, MS
27 source temperature and the mobile phase flow rate (at constant modifier percentage). A
28 factorial experimental design was carried out for this study, which displayed the major and
29 negative role of increased nebulising gas pressure. The factorial design was renewed with the
30 four remaining parameters, allowing to enlighten and explain their different effects on MS
31 responses. Finally, some vegetable oils were analysed by UHPSFC-APCI-HRMS with these
32 optimal conditions to determine the chemical structures of unknown compounds from oily
33 samples.

34

35 **Key words:** Detector response, High Resolution, Hyphenation, Mass spectrometry,
36 Supercritical Fluid Chromatography, Vegetable oil.

37

38 **Highlights:**

- 39 • UHPSFC-APCI-HRMS used for the complete study of vegetable oils
- 40 • No split between UHPSFC and APCI-HRMS for a better sensitivity
- 41 • Understanding of MS parameters on MS responses of lipid compounds
- 42 • Application to Sunflower and *Calophyllum inophyllum* (Tamanu) oils

43

44 **1. Introduction**

45 For several years, Supercritical Fluid Chromatography (SFC) has rapidly grown in
46 analytical chemistry with the introduction of new and more robust SFC (and HPLC/SFC
47 hybrid) systems on the analytical market. Amongst application areas, the lipidomic field
48 draws attention [1–3]. In lipidomics, analytical strategies generally are supported by Gas
49 Chromatography (GC), Normal phase liquid chromatography (NPLC), Non-Aqueous
50 Reversed-Phase Liquid Chromatography (NARP-LC) or Thin-Layer Chromatography (TLC).
51 However, these analytical techniques have encountered several difficulties such as
52 experimental, economic or environmental problems. For instance, the disadvantages of GC
53 are the use of high temperatures for elution, which could favour degradation of thermo-
54 sensitive analytes. Also, in GC, derivatization procedures are time-consuming steps which
55 require methodological developments. TLC (or High Performance TLC) is accurate, fast and
56 versatile but it also requires derivatization agents for lipid detection [2]. Besides, the
57 hyphenation of TLC with MS is not so obvious. Indeed, for this kind of coupling, it is
58 necessary to desorb compounds from the stationary phase. Consequently, several bleeding
59 phenomena may occur that could impact the MS sensitivity. In NARP-LC, only organic and
60 (often) toxic solvents (Acetonitrile (ACN), Methanol (MeOH), Isopropyl alcohol (iPrOH),
61 methylene chloride, or hexane) are used to elute lipids from non-polar stationary phases [4].

62 In SFC, the mobile phase is mainly composed of CO₂ in super/subcritical conditions
63 (depending on the pressure and temperature values, and it has a lower viscosity and a higher
64 diffusivity than liquid mobile phases used in Reversed-Phase-HPLC (RP-LC). Consequently,
65 it is possible to use high flow rates (at least 3 mL/min), while maintaining a high
66 chromatographic efficiency. This green and powerful high-throughput technique has
67 demonstrated a great interest for the screening of complex oily mixtures [1,5,6]. Packed

68 column supercritical fluid chromatography (pcSFC) often improves separations relative to
69 HPLC. It has been successfully applied for the analysis of triacylglycerols (TAG) [7],
70 tocopherols / tocotrienols [8], vitamin D [9], phospholipids, sterols, fatty acids or prenols
71 [5,10] and appears as a good alternative for lipidomics.

72 In SFC, numerous detectors can be used. Closed-cell detectors such as UV detectors can
73 be used but they need to have a pressure-resistant cell. Indeed, the Back-Pressure Regulator
74 (BPR) module that maintains the supercritical state of the mobile phase in the
75 chromatographic system is located after these detectors and this one is set at higher values
76 than the critical value (typically above 12 MPa). Open-cell detectors such as MS, ELSD or
77 Corona Aerosol Detector (CAD) can be directly connected after the BPR without additional
78 interface (when working with short tube length and with modifier mixed or added to CO₂).
79 Indeed, the fluid depressurization provides a natural spray at the detector entrance, which is
80 favourable to these detectors [11].

81 Nowadays, in SFC-MS, the most prevalent MS sources are Atmospheric Pressure
82 Ionisation (API) sources with Electrospray (ESI) and Atmospheric Pressure Chemical
83 Ionization (APCI). During the SFC-MS hyphenation, some difficulties might occur: analyte
84 precipitation in the capillary connector when using low modifier content, carbon ice formation
85 (due to the CO₂ decompression cooling – endothermic reaction- after the BPR), or the lack of
86 adequate solvent to assist the analyte ionization (CO₂ would be inert in ion formation
87 process). However, this technique is gradually introduced in laboratories and is now most
88 commonly used [12]. A make-up solvent is often added (after or before the BPR) to solve
89 some of these problems. This make-up solvent ensures the good solubilisation of compounds
90 after the BPR (for a proper transfer from SFC to MS) and maintains (in most cases) the
91 chromatographic efficiency. Also, it helps to the ion formation (*i.e.* pseudomolecular ion).
92 Moreover, some SFC systems also have a heated BPR. This particularity is very useful (for a
93 direct connection with SFC and MS) to avoid the ice formation or to prevent the compound
94 precipitation as was well explained elsewhere [13,14].

95 In the literature, ESI is the most popular ionization source for SFC-MS due to
96 numerous LC-ESI-MS pharmaceutical applications [14]. The use of a splitter between the
97 column and the ESI source was extensively discussed, especially regarding the interface
98 configuration and the modelling of the splitter behaviour when used with compressible fluids
99 [14]. Today, this trend still continues in the lipidomic field, for polar lipids (phospholipids,
100 glycosylated lipids) [15–19] and pesticides [20]. However, for nonpolar lipids the ESI source
101 may not always be the best choice. In LC, for lipidomic studies, APCI or Atmospheric

102 Pressure Photo-Ionisation (APPI) are complementary to ESI by their specific ionisation
103 mechanisms [8-9]. Some papers related to SFC-APCI-MS [8-9,19] have been published but
104 few of them have demonstrated the influence of SFC and MS parameters on MS responses.
105 Thus, an important gap of fundamental knowledge is highlighted for lipid analysis in SFC-
106 APCI-MS.

107 In the first part of this series of papers [21], we described the effect of the addition of a
108 make-up solvent in terms of location (in relation to the BPR), flow-rate and chemical nature,
109 by using direct Ultra-High-Performance SFC (UHPSFC) coupled to MS with no-split. The
110 direct coupling is expected to favour the MS response with APCI source [22]. Whatever the
111 type of coupling interface, the make-up solvent allowed the introduction of a protic solvent
112 supposedly favouring the ionisation process. However, as was shown, with the use of a
113 mobile phase of CO₂/MeOH (90/10, v/v), we obtained satisfactory responses for lipids from
114 plant seeds without the need for a make-up solvent in a UHPSFC-APCI-MS configuration.

115 The aim of this second part is to have a better understanding of the influence of
116 UHPSFC and MS parameters on MS signals in directly hyphenated UHPSFC-APCI-MS
117 when no additional make-up solvent is used. An oily matrix, extracted by Supercritical Fluid
118 Extraction (SFE) from *Kniphofia uvaria* seeds, which includes fatty acids (FA),
119 diacylglycerols (DAG), hydroxylated TAG (TAG+H₂O), TAG and bioactive (and very minor)
120 anthraquinone (AQ) compounds, was used to study the influence of these parameters. The
121 selected parameters were then applied for a deeper study of sunflower and Calophyllum oils.

122

123 **2. Materials and methods**

124 **2.1 Chemicals**

125 Methanol (MeOH) was purchased from Sigma (St. Quentin Fallavier, France) and it was
126 a reagent grade for LC-MS. For extraction, CO₂ was supplied by Linde (Munich, Germany)
127 with a purity of 99.95%. For UHPSFC-MS analysis, CO₂ was purchased from Messer (Bad
128 Soden, Germany) with a purity of 99.995 %.

129

130 **2.2 Sample preparation of the oily extract by Supercritical Fluid Extraction (SFE)**

131 *Kniphofia uvaria* and Sunflower seeds were collected and prepared at LVMH-
132 Recherche. Seeds of *Kniphofia uvaria* (300 g) were grinded with a Braun blender of 1 L.
133 They were extracted by Supercritical Fluid Extraction (SFE) with a Separex SFE-500

134 apparatus with pure CO₂ for *Kniphofia uvaria* and CO₂/EtOH 97.5/2.5 (v/v) for Sunflower,
135 both at 29 MPa and 60°C. The extraction time depended on the mass of CO₂ eluted through
136 the extraction cell. When the CO₂ mass reached 3 kg, the extraction was stopped. The oil was
137 dried in vacuum with some milliliters of ethanol in order to facilitate the drying. The oil
138 extract was stored at 4°C and under nitrogen to prevent oxidation of compounds. For analysis,
139 the extract was weighed and diluted in MeOH / methylene chloride (1/1, v/v) at 0.1 mg/mL
140 for UHPSFC-HRMS analysis.

141 The *Calophyllum inophyllum* (Tamanu) oil was provided by the French Polynesian
142 University. This oil was stored and prepared for analysis with the same specific protocol as
143 described above.

144

145 **2.3 UHPSFC-HRMS system and analytical conditions**

146 Analytical chromatographic separations were carried out using an equipment purchased
147 from Jasco (Tokyo, Japan) and Thermo-Dionex (Villebon-sur-Yvette, France). The UHPSFC-
148 HRMS system was composed of a CO₂-2080 pump and a back-pressure regulator (BPR) BP-
149 2080 from Jasco and an ultimate 3000 RSLC system (binary pump, autosampler and
150 thermostated column compartment) from Thermo-Dionex [21]. To configure this system, the
151 autosampler controlled the start to run analysis and it was connected by a contact closure to
152 the CO₂ pump. The BPR and CO₂ pump were set to comply with the analysis time with a time
153 program.

154 While previous developments had been conducted on a 75 cm-column (five 15 cm-
155 columns connected in series) to achieve very high efficiency, the present analysis was
156 performed with only one Kinetex C18 column (150 x 4.6 mm, core shell particle 2.6 µm)
157 (Phenomenex, Le Pecq, France) in order to shorten the analysis time (<5 min). The mobile
158 phase was composed of CO₂:MeOH (90/10; v/v) with isocratic elution mode. The column was
159 placed in the LC thermostated column compartment at 9°C [21]. The outlet pressure was
160 equal to 10 MPa and the BPR was thermostated at 70°C. The volume of the BPR was 10 µL.
161 The BPR outlet was directly connected to the MS detector by a simple peek capillary (32 cm
162 x 125 µm). The transfer volume from BPR to MS was 4 µL. MS detection was carried out
163 using a maXis UHR-Q-TOF mass spectrometer (Bruker, Bremen, Germany) in the negative
164 and positive chemical ionisation modes with an APCI source from Bruker. Mass spectra were
165 recorded for *m/z* ranging from 50 to 1400 and the acquisition frequency was 1 Hz in Full Scan
166 mode.

167 At the end of the analysis, the CO₂ pump was turned off and the system depressurized to
168 reach atmospheric pressure. The binary pump continued to deliver 100% MeOH to ensure
169 system equilibration. It was confirmed that no carry-over occurred.

170

171

172 **2.4 Evaluation and optimisation of the SFC and MS conditions by an experimental**

173 **design**

174 The aim of this experimental design was to enhance our knowledge of the SFC-APCI-
175 MS hyphenation. This study identified the most influential parameters on the MS responses
176 for FA, DAG, TAG and two main AQ (rhein and aloe-emodin) included in the oily extract of
177 *Knifophia Uvaria* and selected the best parameter values (from the tested ones) for a lipid
178 screening. As explained in the introduction and in this publication [21], no make-up solvent
179 was necessary to obtain good results. The five variables were: the corona discharge current,
180 the ionisation source temperature, the nebulising gas pressure, the drying gas and the SFC
181 flow rate. Following the recommendations in the user's guide of maXis UHR-Q-TOF mass
182 spectrometer, the following parameters were used: corona discharge (+/- 2µA and +/- 6µA),
183 nebulising gas pressure (N₂) (0.04 and 0.2 MPa), drying gas flow (N₂) (3 and 8 L/min) and
184 drying gas temperature (APCI temperature) included (250 and 450°C). The UHPSFC flow
185 rate was adjusted at 1 and 3 mL/min.

186 Table 1 illustrates the values and their coding for each variable of this experimental
187 design. This factorial design was defined by 35 experiments (Table 2)(2^k with k = 5; 32
188 experimental points and a central point (n°33 with source temperature at 350°C, drying gas
189 flow rate at 5.5 L/min, nebulising gas pressure at 0.12 MPa, SFC flow rate at 2 ml/min and
190 Corona discharge at 4 µA) (done in triplicate) only used for studying the relative standard
191 deviations for peak area (RSD). These RSD were respectively from 3.4 to 7.8% (measured for
192 lipids) and from 3.5 to 4.8% (measured for AQ). These low SD values show the relevance of
193 the experimental design.

194 The responses measured were peak areas of: TAG (LLL and OLL), DAG (LL and OL),
195 FA (linolenic acid) and AQ (anthraquinones with rhein and aloe emodin). The statistical
196 analysis was carried out with Open Office. The values reported in table 3,4 and 5 for the five
197 studied factors are the average values from the 32 experiments, each of the 32 values being
198 calculated as the product of the encoding value -1 or +1 (from table 2) and the experimental
199 peak area.

200 This calculation allows to get negative or positive average values, explaining the
201 respective effect of the lower (negative) or higher (positive) experimental parameters.

203 **2.5 Study of vegetable oil**

204 The analyses of sunflower and Tamanu oil were carried out with optimized SFC-MS
205 conditions by using a total column length of 75 cm to improve the separation quality [7].

208 **3. Results and discussions**

209 **3.1 Understanding the effects of the SFC and MS parameters on MS responses**

210 The negative and positive APCI ionisation modes were used. The effects of different
211 parameters were individually studied for TAG, DAG, FA and AQ families under SFC
212 conditions (CO₂/MeOH, 90/10, v/v). However, in the negative mode, only the AQ family was
213 studied. The carboxylic acid group (for rhein) or alcohol groups (for aloe-emodin) induce a
214 high ionic current by the proton abstraction. Consequently, we decided to use the APCI (+)
215 for an exhaustive analysis and APCI (-) to reveal minor compounds (AQ) not well detected in
216 APCI (+).

218 **3.1.1 Study in SFC-APCI-MS: APCI (+)**

219 **3.1.1.1 First attempt to streamline the SFC-APCI-MS hyphenation**

220 In Fig.1, the peak areas of LLL, OLL, LL, OL (TAG and DAG), linolenic acid and
221 LLL+H₂O (hydroxylated TAG) are plotted for each experiment from the experimental design.
222 Identification of peaks from mass spectra was described in previous papers [21, 23]. Rhein
223 and aloe emodin are not presented in Fig.1 because their peak areas were much lower than
224 other compounds and their MS signals were unobservable with this graphic scale.

225 On Fig. 1, a half of the experiments had no MS responses (or very low MS responses).
226 Thus, one of the experimental parameters has a binary effect on the MS response of lipids,
227 which acts as a switching signal. The variation in the MS response due to the change in the
228 studied parameters was calculated to identify this “binary parameter” (Table 3).

229 As observed in Table 3, the nebulising gas is the key descriptor. This parameter had the
230 highest values (negative) for most of the studied compounds. Thus, the nebulising gas rules
231 this binary trend.

232 For a value fixed at 0.2 MPa (high level), the MS signals dramatically dropped whereas
233 at 0.04 MPa (low level), the MS signals significantly increased. This strong variation in MS
234 responses evidences that the depressurised CO₂ acts as a nebulising gas and is sufficient to
235 ensure the effluent transport by the gaseous phase in the restrictor from the column to the
236 ionization chamber of the mass spectrometer. This effect had already been described in the
237 literature [24]. The high volatility of CO₂ may have assisted the nebulization process for SFC-
238 APCI. Here, the addition of gaseous CO₂ and nebulizing gas (N₂) probably results in too high
239 a rate of compounds in the high wattage chamber at the exit of the spraying needle to allow
240 for good ionization. This high rate of the spray could reduce the compound ionisation by the
241 corona discharge needle in the spray chamber, due to a lower ionisation of the solvent vapor
242 (by removal of an electron). On the other hand, it is more likely that a low transfer of the
243 heaviest compounds into the mass analyser is the reason of this MS response decrease.
244 Indeed, a spray shield (-3.6 kV) is applied for the ion extraction and it could be optimized in
245 order to increase the number of compounds introduced into the MS analyser. Moreover, with
246 this APCI source, the inlet capillary is directed towards the spray needle with an angle of
247 around 120 degrees. This angle obviously favours the ion extraction from the non-ionised
248 compounds but could limit the transfer for heavy compounds (lipids) when a high total gas
249 flow rate (depressurised CO₂ + nebulising gas) is applied. Thus, for lipid analysis, and with
250 the mass spectrometer configuration used in this study, it is necessary to set the nebulising gas
251 pressure at a very low value to improve the MS signals (whatever the SFC flow rate from 1 to
252 3 mL/min).

253 Consequently, in order to improve understanding of the effect of the four remaining
254 parameters, the nebulising gas pressure was set at the lowest value (0.04 MPa) to favour the
255 mass responses. Then, the 16 remaining experiment data were used to perform a new
256 statistical analysis from a reduced set of data (experiments n°1, 2, 3, 4, 9, 10, 11, 12, 17, 18,
257 19, 20, 25, 26, 27 and 28 in Table 2).

258

259 **3.1.1.2 Statistical study relevance for the interpretation**

260

261 Fig. 2 shows the new variations of MS responses related to the four selected factors
262 (ionisation source temperature; drying gas flow rate; SFC flow rate and corona discharge) at a
263 constant low value of the nebulising gas pressure (0.04 MPa). From the reduced data set (16)

264 of the experimental design, a new calculation of the mass response variation was achieved to
265 determine the influence of parameters.

266 Table 4 shows the effect of the four individual factors on the response of selected
267 compounds. However, because there was no central point for this new matrix of data, the
268 validity of the statistical approach is evaluated with a normal probability plot (Henry's graph)
269 (Fig. 3). Henry's line is a tool to check a theoretical distribution. This graph is obtained by
270 plotting the experimental values (product of peak area and encoding value) vs. the centred
271 normalised values (see in legend of figure 3). If the values are perfectly aligned, as is the case
272 here (Fig. 3), the distribution follows a normal distribution. Consequently, this linear
273 distribution allows validating this factorial plan, making it possible to interpret the results
274 with confidence.

275 Table 4 shows that factor 4 (the SFC flow rate) significantly acts on the MS responses
276 for any compound. According to these values, this flow rate is now the first key parameter to
277 optimize for lipids (FA, DAG, TAG). Indeed, it greatly modifies the MS peak area just after
278 the nebulising gas pressure (factor 3 in Table 4). For AQ, this parameter also seems important
279 to optimize but it may be ranked at the third place. The negative values obtained for this
280 parameter indicate that the lowest SFC flow rate value (1 mL/min) will enhance the MS
281 responses. Similar results have already been reported by Hsieh and co-workers [19] for
282 analysis of pharmaceuticals in SFC-APCI-MS by using a total introduction of the mobile
283 phase in MS. They reported that the increase of SFC flow rate from 3 to 6 mL/min had a
284 negative effect on MS responses, which could be due to a less effective heat transfer at higher
285 flow rates.

286 Because ELSD is also an open cell detector, several results obtained in SFC-ELSD
287 could be compared to the SFC-APCI-MS coupling. The first step (the nebulisation process),
288 consisting in mixing the chromatographic eluent with nitrogen (or another gas), is similar in
289 ELSD and APCI-MS detectors. Then, the evaporation of solvent droplets is performed in the
290 drift tube (ELSD) or in the chamber (APCI) at a controlled temperature. One study [25]
291 dealing with the parameter effect on the chromatographic responses in SFC-ELSD also
292 showed that the increase of the SFC flow rate reduced the peak area of caffeine.

293 The ionisation source temperature is described by factor 1 in Table 4. These values are
294 negative for TAG and DAG, but positive for FA and AQ. Thus, for the TAG and DAG
295 analysis in SFC-APCI-MS, it is recommended to use a low APCI temperature (250 °C). This
296 result could be surprising. Indeed, the TAG/DAG boiling points are high so the vaporization
297 process should require a higher temperature. However, TAG and DAG might be thermally

298 fragile analytes and so they could be degraded by high temperature. Other authors have
299 already studied the thermolability properties of glycerides [26,27].

300 Moreover, a TAG analysis by SFC-APCI-MS demonstrated that the APCI temperature
301 was an essential parameter which affected the TAG fragmentation [28]. Consequently, 250°C
302 as APCI temperature seems beneficial to the detection of pseudo-molecular ions. For AQ and
303 FA, the temperature must be set at 450 °C. Hsieh *et al.* [19] published similar results with an
304 APCI source : the rise in temperature had a positive effect on the MS signals. It may be due to
305 a better desolvation of molecules and/or a greater thermal agitation. This last effect
306 would lead to a closer contact between analytes and solvent. Compared to TAG and DAG,
307 AQ and FA possess numerous accessible hydroxyl or acid groups, which can be involved in
308 interactions with the polar MeOH of the mobile phase, resulting in a higher solvation sphere.
309 This hypothesis could explain the behavior of these compounds with relation to the APCI
310 temperature. As reported from these results, the source temperature is also a key parameter
311 (the 3rd parameter to optimize for lipids and 2nd parameter for AQ), which must be optimized
312 depending on the compounds studied.

313 The effect of the APCI corona discharge value is described by factor 5 (Table 4). The
314 corona discharge is an electric discharge (electron emission), which ionizes molecules in the
315 APCI source. These positive values highlight that the use of the highest value for the corona
316 discharge (+6 µA) favour the mass response. Consequently, the increase in discharge current
317 enhances the proportion of ionized molecules in the plasma, enhancing the MS sensitivity.

318 In Table 4, the drying gas flow rate is described by factor 2. These values are negative
319 for all compounds, TAG, DAG and AQ. Thus, the MS optimum signals are achieved for 3
320 L/min. Because the drying gas is opposed to the chromatographic effluent in the MS inlet, the
321 rise in the drying gas flow rate may reduce the proportion of molecules reaching the MS
322 detector. This behaviour could be related to the effect of the nebulising gas previously
323 discussed.

324 However, opposite effects of the drying gas flow rate, obtained with pharmaceutical
325 compounds, were reported in SFC-ESI-MS by using a split and a make-up fluid before the
326 BPR [14,29]. However, according to other previous studies [30], the use of an auxiliary fluid
327 nebulized by an auxiliary gas (N₂) in an interface used with an APCI source and a split
328 configuration enhances the mass response in SFC-MS.

329 Besides, in LC-MS, the drying gas is supposed to favour the reduction of droplets in
330 order to improve the ionisation recovery. However, in UHPSFC-MS, due to the low liquid
331 content in the mobile phase (10% of methanol in this work), the increase in the drying gas

332 flow rate could have an opposite behaviour. This effect may depend on the modifier
333 percentage in the UHPSFC mobile phase, which most often varies from 2 to 50%.

334 In order to better understand how the effects of the analytical parameters are related to
335 the structure of compounds, we can have a look on Ion Mobility Spectrometry (IMS) [31]. In
336 IMS, the separation of analytes that takes place in a gaseous state is ruled by size, shape, and
337 charge. This separation is provided in part by the drift gas (opposite to the MS inlet), and the
338 interaction between ions and the neutral gas is calculated by the Collision Cross-Section
339 (CCS). This CCS depends on structures and three-dimensional conformations. Consequently,
340 molecules with large size (e.g. TAG and DAG) or with planar/rigid 3D conformation (e.g.
341 AQ) may be more affected by the drying gas flow rate, as possibly occurs in the present study
342 after the fluid depressurization.

343 These different conclusions show the effects of mass parameters on the sensitivity,
344 which is strongly related to the conditions, especially the type of ionisation, the use of a split,
345 the addition of a make-up or the total amount of liquid solvent used for the analysis (modifier
346 + make-up solvent), with regards to the size and chemical nature of the studied compounds,
347 and also probably to the ionization source geometry.

348 **3.1.1.3 Summary in APCI (+) for the UHPSFC-MS hyphenation**

349
350 According to this statistical study and to streamline the hyphenation, the first parameter
351 to optimize is the nebulising gas pressure (whatever the analytical conditions). This parameter
352 seems to depend on the type of configuration, the modifier percentage in CO₂ and the amount
353 of make-up solvent delivered. In the present case, there was only 10 % MeOH (isocratic
354 conditions) with direct BPR-MS introduction and no make-up fluid. Consequently, for a lipid
355 analysis (AQ, FA, DAG, TAG) and the use of a small amount of modifier (from 0.1 to 0.3
356 mL/min of MeOH), a low value of nebulising gas pressure is recommended in UHPSFC-
357 APCI-MS (+).

358
359 The UHPSFC flow rate should be studied. For this statistical study, the use of the lowest
360 flow rate (1 mL/min) yielded the optimal MS responses. Thus, for a quantitative lipid
361 analysis, we recommend using a low flow rate to reach the optimal sensitivity or to screen
362 unknown samples. However, a flow rate of 3 mL/min UHPSFC is also possible for the
363 screening of known samples in a high-throughput context. In this case, it could be applied for
364 Quality-Control laboratories (QC lab).

365

366 For a UHPSFC-APCI-MS (+) method development in lipidomics, the APCI temperature
367 will be the next challenge. This parameter should be optimized in function of the heat-
368 resistance and chemical structure of the targeted compounds. This lipid analysis of TAG and
369 DAG highlighted that the lowest temperature values (250°C) should be favoured, whereas for
370 AQ and FA, 450°C was the best APCI temperature. Consequently, for a first lipid screening
371 (with a low MeOH amount from 0.1 to 0.3 mL per min) and to obtain an exhaustive response,
372 we recommend using a low APCI temperature. Indeed, several molecular families have
373 structural similarities with DAG and TAG as for instance phospholipids, glycolipids etc...
374 and as shown in [21], this strategy would permit to ensure a fast and reliable response.

375

376 Finally, based on this lipid strategy, the analytical conditions selected in the following
377 sections 3.2 and 3.3 are: source temperature 450°C (to detect bioactive and minor polar
378 compounds), nebulising gas 0.04 MPa, and UHPSFC flow rate 1 mL/min, with 10% MeOH.
379 Thus, satisfactory results are obtained with both of the other two parameters: the corona
380 values (2 and 6 μ A) and the drying gas flow rate (3 and 8 L/min). This means that these two
381 parameters are not as significant as the three previous ones. We thus selected a high corona
382 value (6 μ A) and a low drying gas flow rate (3 L/min) to favour the mass responses for minor
383 and polar AQ compounds.

384

385 Figure 4 shows the area differences measured for LLL and OLL at 250°C and 0.04 MPa
386 (optimal MS responses of TAG). Whatever the drying gas flow rate (3 or 8 L/min) and the
387 corona value (2 and 6 μ A), the response differences are reduced at high mobile phase flow
388 rate (3 mL/min) whereas they are greater at low mobile phase flow rate (1 mL/min). It clearly
389 shows that the ionisation recovery, which is related to the compound structure (here these two
390 TAGs differ by one double bond) is dramatically different with regards to the mobile phase
391 flow rate.

392

393 **3.1.2 Study in UHPSFC-APCI-MS: APCI (-)**

394 The negative mode in APCI was applied to study the AQ family because a higher MS
395 response was obtained in APCI (-) for these hydroxylated or acidic compounds.

396 Table 5 describes the effect of the five individual factors on the MS response (peak
397 area) for rhein and aloe emodin. According to this table, the drying gas flow rate (factor 2) is

398 the first parameter to optimize in a method development. Thus, 3 L/min as drying gas flow
399 rate should be selected (negative values).

400 It is difficult to rank the other parameters. However, these data may be interpreted. The
401 APCI temperature is illustrated by factor 1. It is necessary to apply a high APCI temperature
402 (450°C) to improve ionisation efficiency. Corona current (factor 5) and nebulising gas
403 pressure (factor 3) parameters should be respectively fixed at 6 μ A and 0.04 MPa. These
404 results are consistent with the above study in APCI (+), despite a different ionisation
405 mechanism. However, the UHPSFC flow rate (factor 4) has a different impact for the AQ
406 detection. Therefore a UHPSFC flow rate of 3 mL/min should be set up for aloe emodin and 1
407 mL/min for rhein. These opposite effects of the UHPSFC flow rate for rhein and aloe emodin
408 in APCI (-) could be related to the different chemical structure between aloe emodin
409 (hydroxyl group) and rhein (carboxylic group), which react differently. Differential
410 behaviours in the effect of the UHPSFC flow rate on the MS response in UHPSFC-APCI-MS
411 were also reported in the analysis of cytarabine and clofazimine in mouse plasma [32].

412

413 **3.2 Application to sunflower oil in UHPSFC-APCI-MS (+)**

414 Sunflower oil is often used in cosmetics as a component of the formulations or as a
415 green extraction solvent to extract various active compounds from plants. Thus, to evaluate
416 the extraction recovery, the study of the vegetable oil composition should be achieved.

417 Figure 5 shows the chromatograms for a sunflower oil, obtained by SFE or by cold-
418 pressed extraction. Between 40 and 80 minutes, the TAG composition shows some
419 composition differences between the two samples. This SFE extraction seems to have
420 favoured the recovery of the most unsaturated TAG, *i.e.* LLL, PLL, OLL, or OOL, whereas
421 cold-pressed extraction favours the recovery of the most saturated species, POO, OOO and
422 SOO. This result is not unexpected due to the use of 2.5% ethanol in CO₂ for the SFE extract,
423 which induces a higher solubility of TAG having double bonds in the alkyl chains.

424 The most surprising is the presence of several peaks between 30 and 40 minutes for the
425 SFE extract. The MS identification for one of the major peaks was achieved by the study of
426 the mass spectrum (Fig. 6). The peak at m/z 896.73984 is due to [LLL(OH)+H]⁺ whereas the
427 peak at m/z 877.72926 corresponds to the loss of a water molecule from the previous one.
428 These peaks show that the SFE extraction favoured the recovery of hydroxylated triglycerides
429 with regards to cold-pressed extraction.

430

431 **3.3 Application to *Calophyllum inophyllum* oil (Tamanu oil) in UHPSFC-APCI-MS (+)**

432 The UHPSFC-HRMS-APCI (+) coupling was also applied to the *Calophyllum*
433 *inophyllum* oil, which is used in topical application by Polynesians, or as a traditional
434 medicine ingredient or as a well-being ingredient [33, 34]. This analysis was achieved at
435 450°C (for the mass source) to improve the response of the first eluted peaks, but this was
436 detrimental to the peak area of TAG due to a probable thermo-sensitivity of the tri-esters (Fig.
437 7).

438 Figure 7 shows three peak areas. Between 40 and 80 minutes, the TAG found in this oil
439 were in accordance with previous reports [35,36]. DAG eluted around 20 minutes whereas
440 several compounds eluted around 10 minutes, in which the following were identified:
441 Tamanolide (C₂₄H₂₈O₅), Calophyllolide (C₂₅H₂₂O₅), and Inophyllum (E or C) (C₂₅H₂₀O₅).
442 These three compounds were previously reported in Tamanu oil ethanolic extracts [34], *i.e.* an
443 extract free of the main lipids. The analysis of these ethanolic extracts was achieved with
444 normal phase liquid chromatography, with a mobile phase composed of cyclohexane-
445 ethylacetate and a silica gel stationary phase [34]. The UHPSFC approach allows a most
446 complete oil analysis, including both lipid composition and the study of the main bioactive
447 compounds, without fractionation of the ethanol-soluble compounds. However, the separation
448 of some isomers (Inophyllum C and E) was not reached with these C18 stationary phases in
449 UHPSFC, and an improvement of this separation should be performed in the future.

450

451 **4. Conclusions**

452 The direct coupling of UHPSFC to the APCI-MS interface has showed a great potential
453 for lipid analyses of various matrices containing bioactive compounds (ex: AQ, coumarins)
454 with a mixture of methanol and CO₂ in isocratic conditions. The positive and negative
455 ionisation mode were studied. The main advantages of this kind of direct hyphenation
456 (UHPSFC to MS with no split) is to have a better MS sensitivity without losing the
457 chromatographic resolution of the MS peak (on condition of working with an optimised BPR
458 design).

459 As described in section 3.1.2, for UHPSFC method development in APCI (+) focused
460 on lipids, the nebulising gas pressure had a dramatic effect on the MS responses. Due to this
461 direct interface by the introduction of the total flow in the APCI source, this pressure should
462 be set at the lowest value. In addition, the mobile phase and the drying gas flow rates should
463 both be reduced to improve the sensitivity. Besides, the ionisation source temperature also had

464 an impact, but this parameter must be optimized for each targeted compound. In our case, this
465 parameter was related to a probable thermo-sensitivity of the lipid esters. As usually observed,
466 the increase in the corona discharge value enhanced peak area for all compounds.

467 The negative APCI mode favoured the MS response for AQ with regards to the positive
468 mode, but the lipid part of the oil could not be observed. Consequently, this ionisation mode
469 will permit to have a better sensitivity and selectivity for some compounds and it will be used
470 in a second approach.

471 With the UHPSFC-APCI-HRMS, we could elucidate chemical structures ($\Delta < 2$ ppm)
472 and screen several raw materials for the cosmetic field to detect minor bioactive compounds.
473 We showed the presence of hydroxylated TAG in sunflower oil and this approach could be
474 useful for a better total characterisation of the *Calophyllum inophyllum* oil.

475

476 Acknowledgments.

477

478 The authors want to warmly thank Prof. P. Raharivelomanana, UMR 241, Université de la
479 Polynésie Française (UPF) for the gift of the Tamanu oil sample, and V. Pecher, LVMH
480 Recherche, Saint Jean de Braye, for the gift of the *Knifophia Uvaria* seeds.

Figure captions

Figure 1: Descriptive analysis of 33 experiments from the experimental design in function of FA, DAG, TAG molecular mass from a *Kniphofia uvaria* oily extract (0.5 mg/mL) – Analytical conditions: 1 Kinetex C18 column (150 x 4.6 mm, 2.7 μ m), 9°C, 10 MPa, $V_{inj} = 5 \mu$ L.

Figure 2: Descriptive analysis of 16 experiments from the experimental design in function of TAG, DAG, FA molecular mass from a *Kniphofia uvaria* oily extract (0.5 mg/mL) – see Fig. 1 for analytical conditions.

Figure 3: Evaluation of the distribution of experimental results (from 16 experiments) performed by the Henry graph for each compound. x axis: product of the experimental peak area and the encoding value (-1 or +1) ; y axis: normalized data ($y = (x - x_{average})/\sigma$)

Figure 4: The MS response peak area differences between LLL and OLL in UHPSFC-HRMS-APCI (+) according to varied analytical conditions (drying gas flow rate, mobile phase flow rate, corona discharge) applied in APCI-MS with a source temperature equal to 250°C.

Figure 5: Chromatographic profile of sunflower oil analysed by UHPSFC-HRMS-APCI (+). For analytical conditions see in Text. Green chromatogram: oil obtained from mechanical cold pressure; Orange chromatogram: oil obtained from SFE extraction (see conditions in the text).

Figure 6: Mass spectra of the main additional peak obtained by SFE for the sunflower oil (see pink arrow in Fig. 5). Columns: 4 Kinetex C18 + 1 Accucore C18 (each with dimensions of 150 mm x 4.6 mm; particle size respectively 2.7 and 2.6 μ m); Mobile phase: CO₂/MeOH (90/10; v/v); T°C = 9°C; P_{out} = 10 MPa; F = 1 ml/min. HRMS-APCI+: T° = 450°C; corona discharge value = +6 μ A; 0.04 MPa (N₂); Drying gas flow rate = 3 L/min; $V_{inj} = 5 \mu$ L, oil concentration = 0.1 mg/ml dissolved in MeOH/CH₂Cl₂ (50/50, v/v).

Figure 7: Chromatogram of *Calophyllum inophyllum* oil by UHPSFC-HRMS-APCI+. Columns: 4 Kinetex C18 + 1 Accucore C18 (each with dimensions of 150 mm x 4.6 mm; particle size respectively 2.7 and 2.6 μ m); Mobile phase: CO₂/MeOH (90/10; v/v); T°C =

9°C; $P_{\text{out}} = 10 \text{ MPa}$; $F = 1 \text{ ml/min}$. HRMS-APCI+: $T^\circ = 450^\circ\text{C}$; corona discharge value = +6 μA ; 0.04 MPa (N_2); Drying gas flow rate = 3 L/min; $V_{\text{inj}} = 5 \mu\text{L}$, oil concentration = 0.1 mg/ml dissolved in MeOH/ CH_2Cl_2 (50/50, v/v).

Tables

Table 1: Experimental design

Table 2: Variable encoding for the experimental design (see significance of -1 and +1 values in table 1). For experiment 33, the 0 encoding values correspond to 350° for source temperature; 5.5 L/min for drying gas; 0.12 MPa for Nebulising gas; 2 ml/min for SFC flow rate, and 4 µA for corona discharge).

Table 3: Average values obtained from the products of the peak area and the encoding value (-1; +1) of the parameter for the anthraquinones (Rhein, Aloe emodin) and the lipidic compounds (Linolenic acid, LL, OL, LLL+ H₂O, LLL,OLL) for the 32 experiments. Analytical conditions: 1 Kinetex C18 column (150 x 4.6 mm, 2.7 µm), 9°C, 10 MPa, 5 µL, APCI+.

Table 4: Average values from the products of the peak area and the encoding value of the parameter for the anthraquinones (Rhein, Aloe emodin) and the lipidic compounds (Linolenic acid, LL, OL, LLL+ H₂O, LLL,OLL) for 16 experiments with a nebulizing gas equal to 0.04 MPa Analytical conditions identical to table 3.

Table 5: Average values obtained from the products of the peak area and the encoding value (-1; +1) of the parameter for the anthraquinones (Rhein, Aloe emodin) for the 32 experiments. Analytical conditions: 1 Kinetex C18 column (150 x 4.6 mm, 2.7 µm), 9°C, 10 MPa, 5 µL; APCI-.

5. References

- [1] L. Laboureur, M. Ollero, D. Touboul, Lipidomics by Supercritical Fluid Chromatography, *Int. J. Mol. Sci.* 16 (2015) 13868–13884.
- [2] R.E. McDonald, M.M. Mossoba, *New Techniques and Applications in Lipid Analysis*, AOCS Press, 1997. <https://books.google.fr/books?id=Az--ViqODWMC>.
- [3] E. Lesellier, Analysis of non-saponifiable lipids by super-/subcritical-fluid chromatography, *J. Chromatogr. A.* 936 (2001) 201–214.
- [4] M. Holčápek, P. Jandera, P. Zderadička, L. Hrubá, Characterization of triacylglycerol and diacylglycerol composition of plant oils using high-performance liquid chromatography–atmospheric pressure chemical ionization mass spectrometry, *J. Chromatogr. A.* 1010 (2003) 195–215.
- [5] M. Lísa, M. Holčápek, High-Throughput and Comprehensive Lipidomic Analysis Using Ultrahigh-Performance Supercritical Fluid Chromatography–Mass Spectrometry, *Anal. Chem.* 87 (2015) 7187–7195.
- [6] J. Duval, C. Colas, V. Pecher, M. Poujol, J.-F. Tranchant, É. Lesellier, Contribution of Supercritical Fluid Chromatography coupled to High Resolution Mass Spectrometry and UV detections for the analysis of a complex vegetable oil – Application for characterization of a *Kniphofia uvaria* extract, *Cosmetopoeia Cosmétopée*. 19 (2016) 1113–1123.
- [7] E. Lesellier, A. Latos, A.L. de Oliveira, Ultra high efficiency/low pressure supercritical fluid chromatography with superficially porous particles for triglyceride separation, *J. Chromatogr. A.* 1327 (2014) 141–148.
- [8] M. Méjean, A. Brunelle, D. Touboul, Quantification of tocopherols and tocotrienols in soybean oil by supercritical-fluid chromatography coupled to high-resolution mass spectrometry, *Anal. Bioanal. Chem.* 407 (2015) 5133–5142.
- [9] F. Jumaah, S. Larsson, S. Essén, L.P. Cunico, C. Holm, C. Turner, M. Sandahl, A rapid method for the separation of vitamin D and its metabolites by ultra-high performance supercritical fluid chromatography–mass spectrometry, *J. Chromatogr. A.* 1440 (2016) 191–200.
- [10] L.-F. Nothias, S. Boutet-Mercey, X. Cachet, E.D.L. Torre, L. Laboureur, J.-F. Gallard, P. Retailleau, A. Brunelle, P.C. Dorrestein, J. Costa, L.M. Bedoya, F. Roussi, P. Leysen, J. Alcami, J. Paolini, M. Litaudon, D. Touboul, Environmentally Friendly Procedure Based on Supercritical Fluid Chromatography and Tandem Mass Spectrometry Molecular Networking for the Discovery of Potent Antiviral Compounds from *Euphorbia semiperfoliata*, *J. Nat. Prod.* 80 (2017) 2602–2608.
- [11] E. Lesellier, C. West, The many faces of packed column supercritical fluid chromatography – A critical review, *Ed. Choice IX. J. Chromatogr. A* 1382 (2015) 2–46.
- [12] C. West, Current trends in supercritical fluid chromatography, *Anal. Bioanal. Chem.* 410(2018)6441–6457

- [13] A. Tarafder, Designs and methods for interfacing SFC with MS, *J. Chromatogr. B* 1091 (2018) 1–13.
- [14] A.G.-G. Perrenoud, J.-L. Veuthey, D. Guillarme, Coupling state-of-the-art supercritical fluid chromatography and mass spectrometry: from hyphenation interface optimization to high-sensitivity analysis of pharmaceutical compounds, *J. Chromatogr. A* 1339 (2014) 174–184.
- [15] T. Bamba, N. Shimonishi, A. Matsubara, K. Hirata, Y. Nakazawa, A. Kobayashi, E. Fukusaki, High throughput and exhaustive analysis of diverse lipids by using supercritical fluid chromatography-mass spectrometry for metabolomics, *J. Biosci. Bioeng.* 105 (2008) 460–469.
- [6] K. Hori, A. Matsubara, T. Uchikata, K. Tsumura, E. Fukusaki, T. Bamba, High-throughput and sensitive analysis of 3-monochloropropane-1, 2-diol fatty acid esters in edible oils by supercritical fluid chromatography/tandem mass spectrometry, *J. Chromatogr. A* 1250 (2012) 99–104.
- [17] J.W. Lee, S. Nishiumi, M. Yoshida, E. Fukusaki, T. Bamba, Simultaneous profiling of polar lipids by supercritical fluid chromatography/tandem mass spectrometry with methylation, *J. Chromatogr. A* 1279 (2013) 98–107.
- [18] J.W. Lee, T. Uchikata, A. Matsubara, T. Nakamura, E. Fukusaki, T. Bamba, Application of supercritical fluid chromatography/mass spectrometry to lipid profiling of soybean, *J. Biosci. Bioeng.* 113 (2012) 262–268.
- [19] Y. Hsieh, L. Favreau, K. Cheng, J. Chen, Chiral supercritical fluid chromatography/tandem mass spectrometry for the simultaneous determination of pindolol and propranolol in metabolic stability samples, *Rapid Commun. Mass Spectrom.* 19 (2005) 3037–3041.
- [20] Y. Fujito, Y. Hayakawa, Y. Izumi, T. Bamba, Importance of optimizing chromatographic conditions and mass spectrometric parameters for supercritical fluid chromatography/mass spectrometry, *J. Chromatogr. A* 1508 (2017) 138-187.
- [21] J. Duval, C. Colas, V. Pecher, M. Poujol, J.-F. Tranchant, E. Lesellier, Hyphenation of ultra-high performance supercritical fluid chromatography with atmospheric pressure chemical ionisation high resolution mass spectrometry: Part 1. Study of the coupling parameters for the analysis of natural non-polar compounds, *J. Chromatogr. A* 1509 (2017) 132–140.
- [22] J. Duval, C. Colas, V. Pecher, M. Poujol, J.F. Tranchant, E. Lesellier, Contribution of supercritical fluid chromatography coupled to high resolution mass spectrometry and UV detection for the analysis of complex vegetable oil. Application for the characterization of the *Kniphofia uvaria* extract, *C.R. Chimie* 19(2016)117

- [23] D. Guillaume, V. Desfontaine, S. Heinisch, J.L. Veuthey, What are the current solutions for interfacing supercritical fluid chromatography and mass spectrometry, *J. Chromatogr. B*, 1083 (2018) 160-170
- [24] F. Li, Y. Hsieh, Supercritical fluid chromatography – mass spectrometry for chemical analysis, *J. Sep. Sci.* 31 (2008) 1231-1237.
- [25] E. Lesellier, A. Valarché, C. West, M. Dreux, Effects of selected parameters on the response of the evaporative light scattering detector in supercritical fluid chromatography, *J. Chromatogr. A* 1250 (2012) 220–226.
- [26] D. Bradin, Thermal decomposition process of triglyceride containing mixtures, co-processed with low molecular weight olefins to produce a renewable fuel composition, US8841494B2.
- [27] A. Crossley, T.D. Heyes, B.J.F. Hudson, The effect of heat on pure triglycerides, *J. Am. Oil Chem. Soc.* 39 (1962) 9–14.
- [28] B.C. Byrdwell, Atmospheric Pressure Chemical Ionization Mass Spectrometry for Analysis of Lipids, *Lipids* 36 (2001) 327-346.
- [29] J. Prothmann, M. Sun, P. Spégel, M. Sandhal, C. Turner, Ultra High performance of supercritical fluid chromatography with quadrupole-time-of-flight mass spectrometry (UHPSFC/QTOF-MS) for analysis of lignin-derived monomeric compounds in processed lignin samples, *Anal. Bioanal. Chem.* 409 (2017) 7049-7061.
- [30] M.C. Ventura, W.P. Farrell, C. M. Aurigemma, M.J. Greig, Packed column supercritical fluid chromatography/mass spectrometry for high-throughput analysis. Part2, *Anal. Chem.* 71 (1999) 4223-4231.
- [31] G.A. Eiceman, Z. Karpas, H.H. Hill, *Ion Mobility Spectrometry*, Third Edition, Taylor & Francis, 2013. <https://books.google.fr/books?id=tnlcAgAAQBAJ>.
- [32] Y. Hsieh, F. Li, C. J. G. Duncan, Supercritical Fluid Chromatography and High-Performance Liquid Chromatography/Tandem Mass Spectrometric Methods for the Determination of Cytarabine in Mouse Plasma, *Anal. Chem.* 79 (2007) 3856-3861.
- [33] A.C. Dweck, T. Meadows, Tamanu (*Calophyllum inophyllum*) - the African, Asian, Polynesian and Pacific Panacea, *Int. J. Cosmet. Sci.* 24 (2002) 341-348.
- [34] J.L. Ansel, E. Lupo, L. Mijouin, S. Guillot, J.F. Butaud, R. Ho, G. Lecellier, P. Raharivelomanana, C. Pichon, Biological Activity of Polynesian *Calophyllum inophyllum* Oil Extract on 6 Human Skin Cells, *Planta Med.* 82 (2016) 961-966.
- [35] E. Lesellier, A. Tchaplal, Retention Behavior of Triglycerides in Octadecyl Packed Subcritical Fluid Chromatography with CO₂/Modifier Mobile Phases, *Anal. Chem.* 71 (1999) 5372–5378.

[36] E. Lesellier, J. Bleton, A. Tchaplà, Use of relationships between retention behaviors and chemical structures in subcritical fluid chromatography with CO₂/modifier mixtures for the identification of triglycerides, *Anal Chem.* 72 (2000) 2573-2580.

| Factor | Definition | Low value (-1) | High value (+1) |
|--------|------------------------------------|----------------|-----------------|
| 1 | Ionisation source temperature (°C) | 250 | 450 |
| 2 | Drying gas (L/min) | 3 | 8 |
| 3 | Nebulising gas (MPa) | 0.04 | 0.2 |
| 4 | SFC flow (mL/min) | 3 | 1 |
| 5 | Corona (mA) | 2 | 6 |

Table 1

| Experiment | Ionisation source temperature (APCI) (°C) | Drying gas (L/min) | Nebulising gas (MPa) | SFC flow (mL/min) | Corona (µA) |
|------------|---|--------------------|----------------------|-------------------|-------------|
| 1 | -1 | -1 | -1 | -1 | -1 |
| 2 | -1 | -1 | -1 | -1 | +1 |
| 3 | -1 | -1 | -1 | +1 | -1 |
| 4 | -1 | -1 | -1 | +1 | +1 |
| 5 | -1 | -1 | 1 | -1 | -1 |
| 6 | -1 | -1 | 1 | -1 | +1 |
| 7 | -1 | -1 | 1 | +1 | -1 |
| 8 | -1 | -1 | 1 | +1 | +1 |
| 9 | -1 | +1 | -1 | -1 | -1 |
| 10 | -1 | +1 | -1 | -1 | +1 |
| 11 | -1 | +1 | -1 | +1 | -1 |
| 12 | -1 | +1 | -1 | +1 | +1 |
| 13 | -1 | +1 | 1 | -1 | -1 |
| 14 | -1 | +1 | 1 | -1 | +1 |
| 15 | -1 | +1 | 1 | +1 | -1 |
| 16 | -1 | +1 | 1 | +1 | +1 |
| 17 | +1 | -1 | -1 | -1 | -1 |
| 18 | +1 | -1 | -1 | -1 | +1 |
| 19 | +1 | -1 | -1 | +1 | -1 |
| 20 | +1 | -1 | -1 | +1 | +1 |
| 21 | +1 | -1 | 1 | -1 | -1 |
| 22 | +1 | -1 | 1 | -1 | +1 |
| 23 | +1 | -1 | 1 | +1 | -1 |
| 24 | +1 | -1 | 1 | +1 | +1 |
| 25 | +1 | +1 | -1 | -1 | -1 |
| 26 | +1 | +1 | -1 | -1 | +1 |
| 27 | +1 | +1 | -1 | +1 | -1 |
| 28 | +1 | +1 | -1 | +1 | +1 |
| 29 | +1 | +1 | 1 | -1 | -1 |
| 30 | +1 | +1 | 1 | -1 | +1 |
| 31 | +1 | +1 | 1 | +1 | -1 |
| 32 | +1 | +1 | 1 | +1 | +1 |
| 33 | 0 | 0 | 0 | 0 | 0 |

Table 2

| | Rhein | Aloe emodin | Linolenic acid | LL | OL | LLL+H ₂ O | LLL | OLL |
|--------------------|--------|-------------|----------------|------------|-----------|----------------------|------------|------------|
| Source temperature | 6 916 | 15 795 | 36 205 | -1 118 818 | -987 628 | 39 846 | -800 203 | -1 032 659 |
| Drying gas | -3514 | -2175 | 13113 | -144 150 | -102 884 | -489 059 | -544 015 | -539 312 |
| Nebulising gas | -5 761 | -12 152 | -81 306 | -3 002 108 | -266 0372 | -3 251 657 | -4 812 258 | -3 311 593 |
| SFC flow rate | -4 560 | -11 196 | -39 464 | -1 212 755 | -352 486 | -802 373 | -1 863 651 | -1 343 699 |
| Corona discharge | 1 777 | 4 196 | 11 692 | 413 659 | 347 223 | 175 412 | 802 329 | 699 808 |

Table 3

| | Rhein | Aloe emodin | Linolenic acid | LL | OL | LLL+H ₂ O | LLL | OLL |
|--------------------|--------|-------------|----------------|------------|------------|----------------------|------------|------------|
| Source temperature | 12 676 | 27 947 | 61 842 | -2 279 823 | -2 011 281 | -24 124 | -1 831 241 | -2 201 975 |
| Drying gas | -8 133 | -7 994 | 14 564 | -372 909 | -303 673 | -1 067 344 | -1 296 931 | -1 206 690 |
| SFC flow rate | -7 866 | -18 802 | -83 744 | -2 502 880 | -806 069 | -1 699 192 | -3936921 | -2 816 809 |
| Corona discharge | 2 399 | 4 749 | 19 841 | 790 520 | 659 953 | 316 666 | 1 533 559 | 1 359 095 |

Table 4

| | Rhein | Aloe emodin |
|--------------------|----------|-------------|
| Source temperature | 138 214 | 159 212 |
| Drying gas | -207 151 | -2 177 873 |
| Nebulising gas | -78 034 | -533 165 |
| SFC flow rate | -82 257 | 606 331 |
| Corona discharge | 18 547 | 201 154 |

Table 5

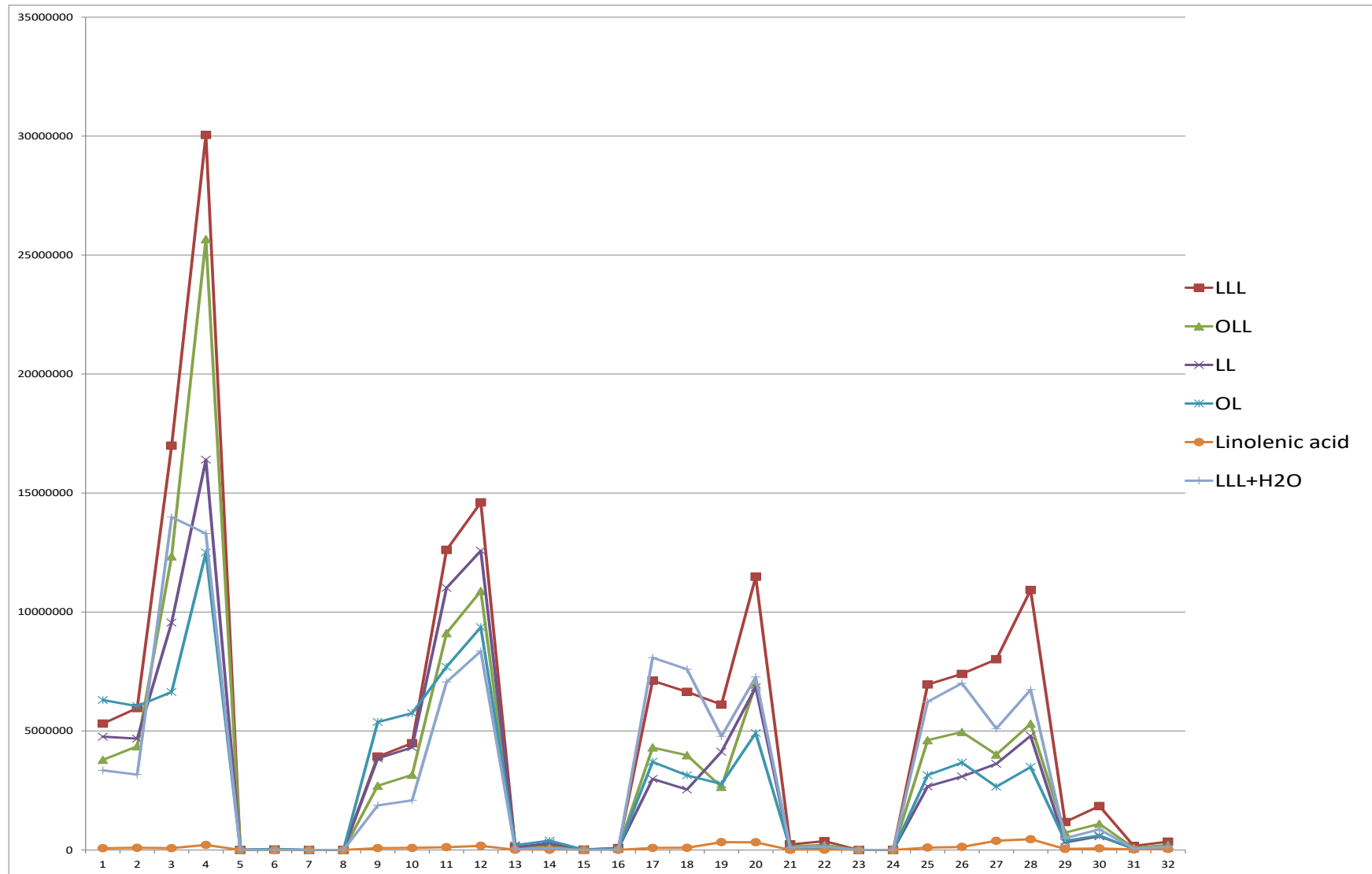


Figure 1

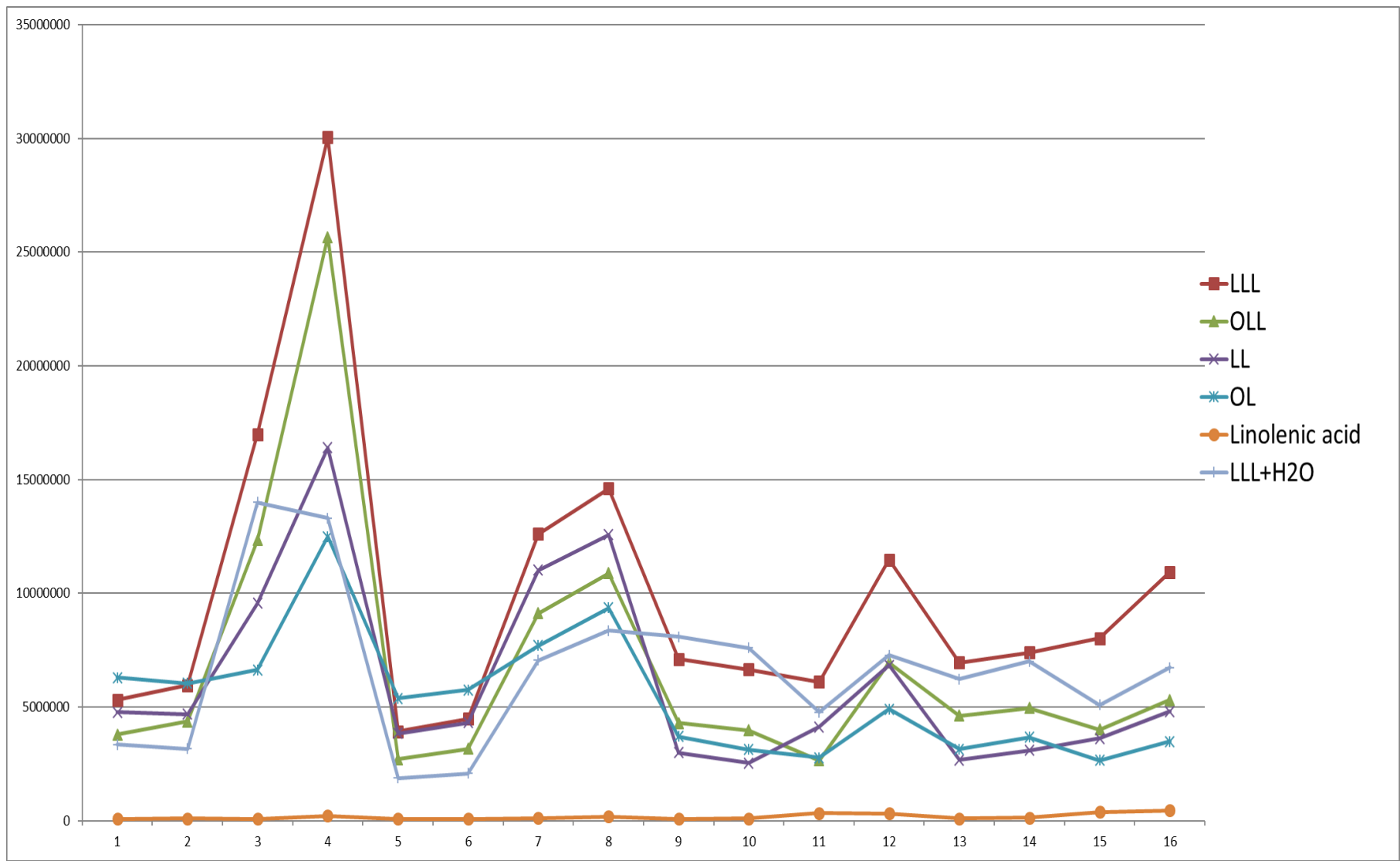


Figure 2

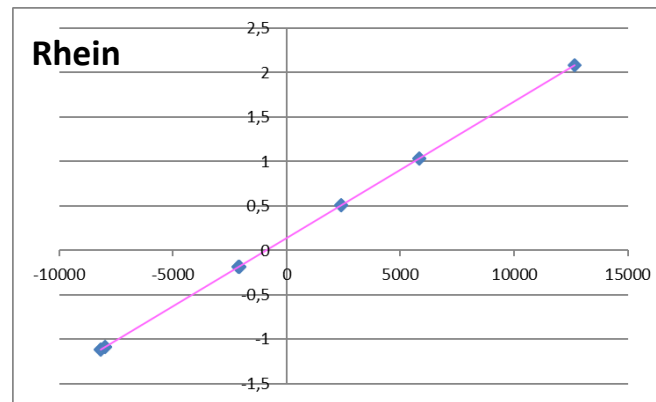
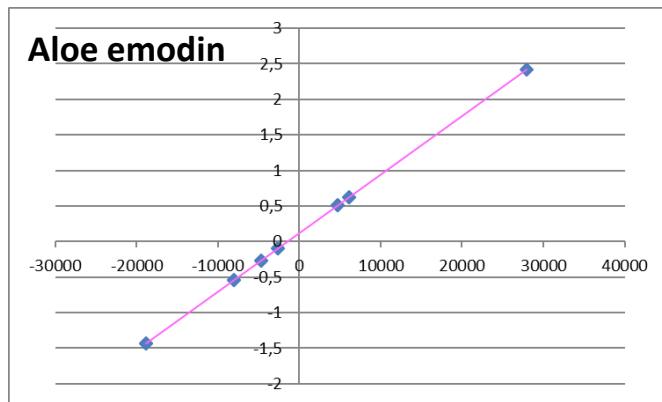
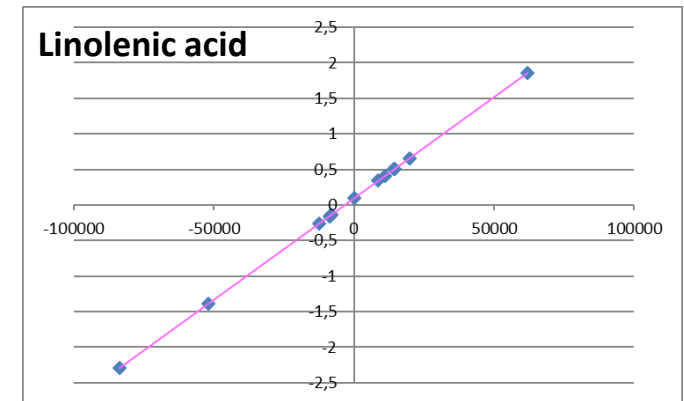
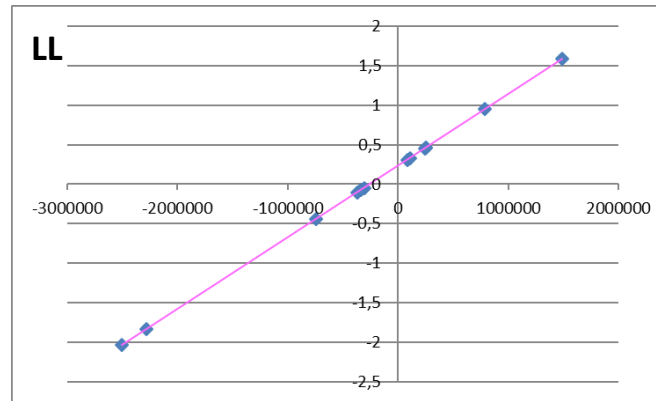
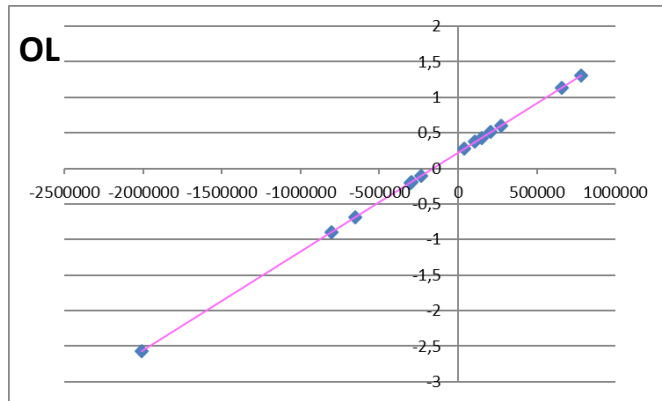
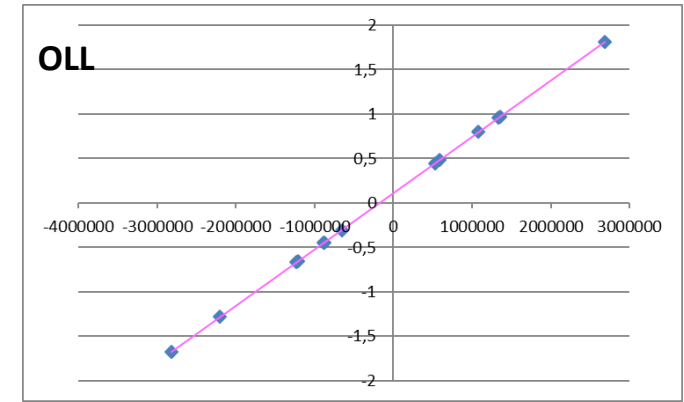
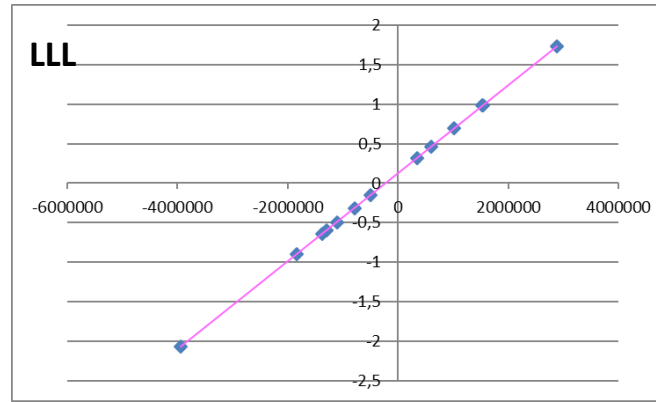
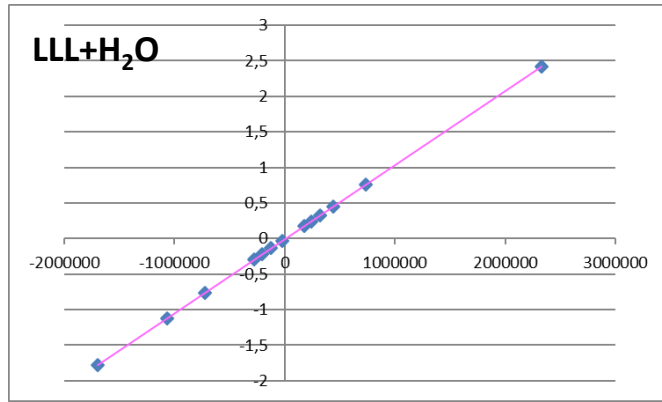


Figure 3

Peak area difference

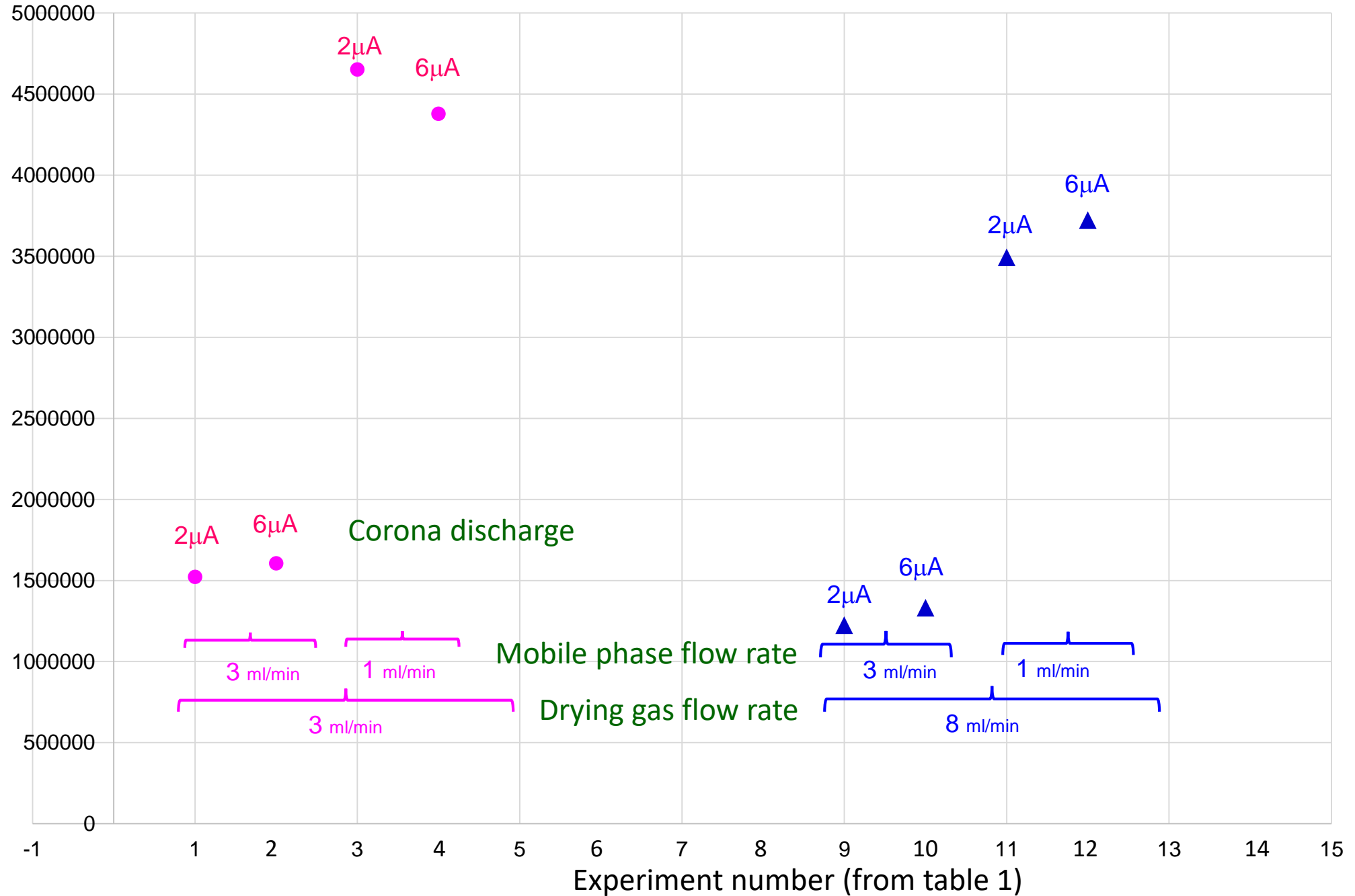


Figure 4

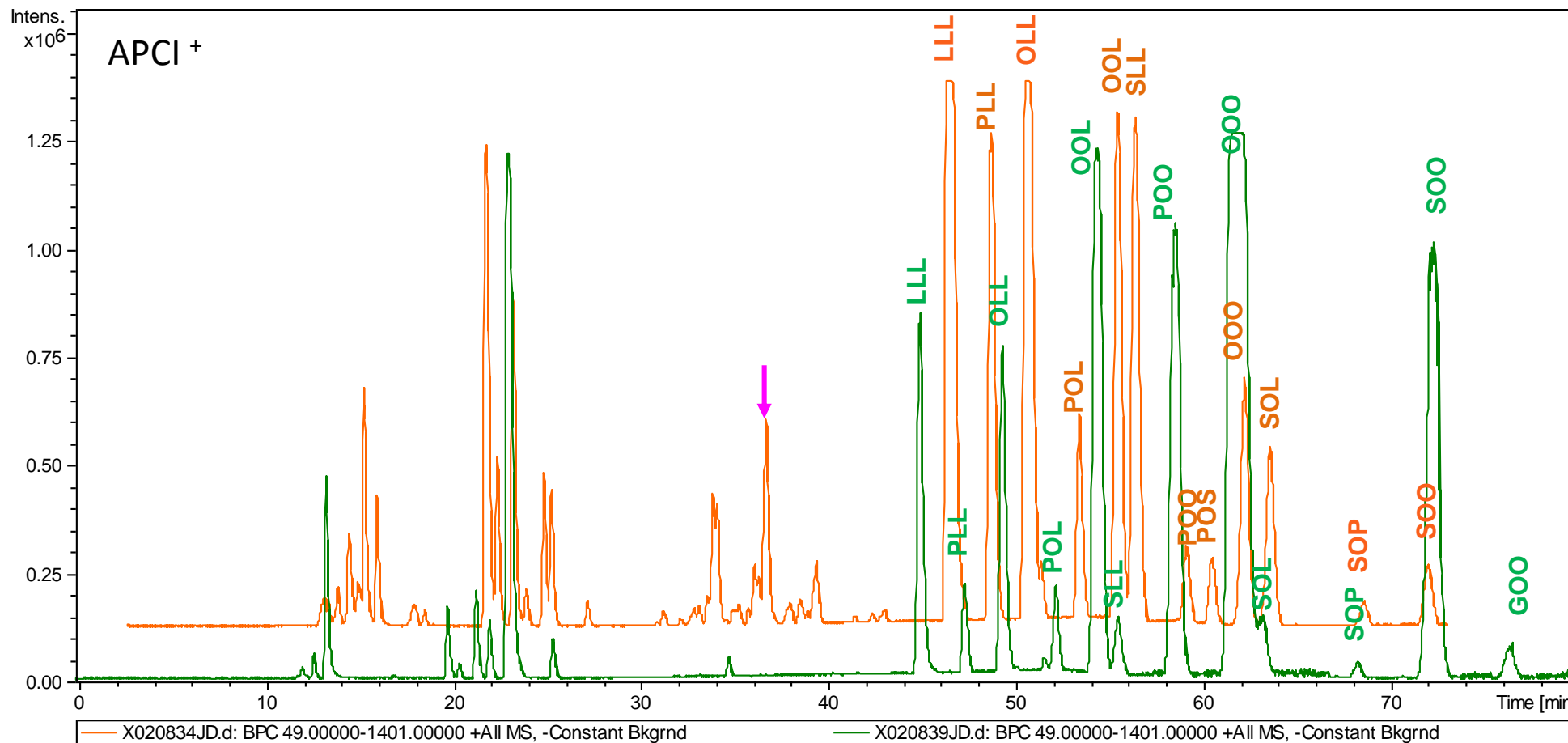


Figure 5

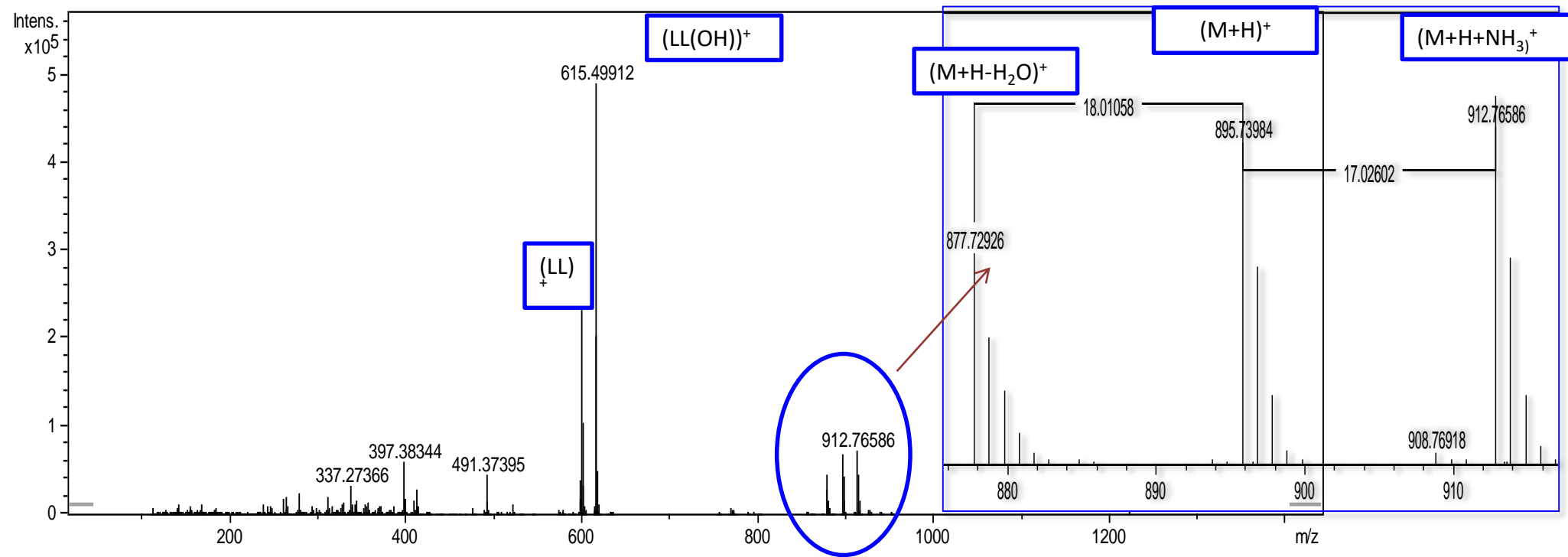


Figure 6

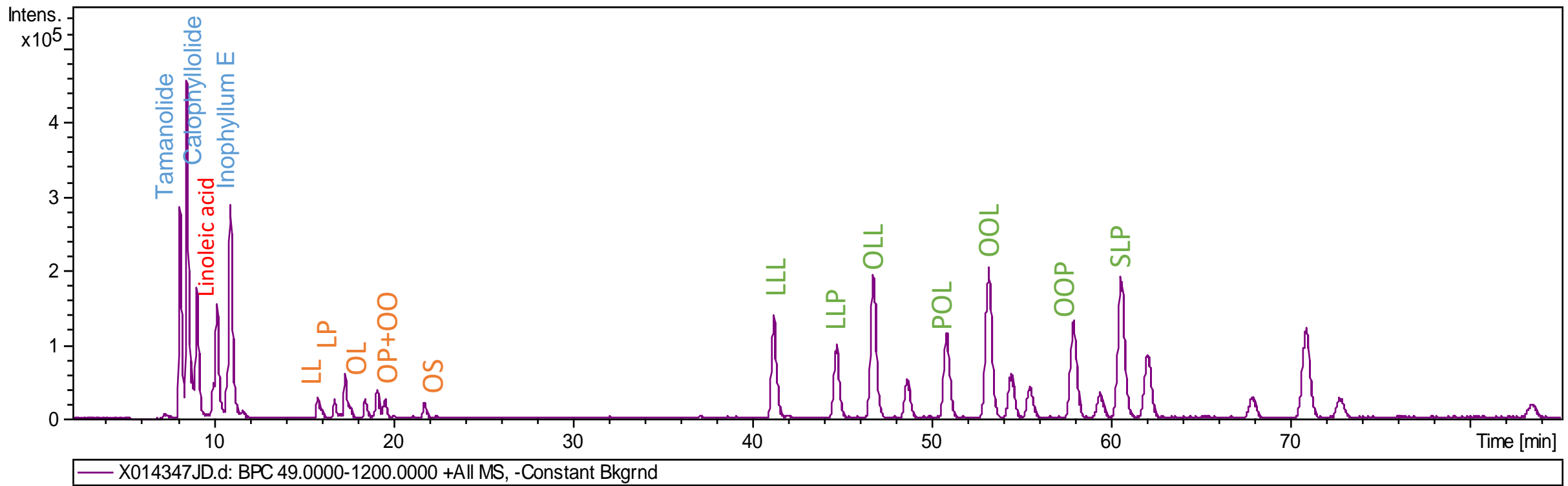


Figure 7